Green and Facile Approach for the Synthesis of ZnO/MgO Nanocomposite using *Azadirachta indica* Leaf Extract: Characterization and Photocatalytic Activity

Dwivedi Poonam*, Satiya Honey and Jatrana Indu
Department of Chemistry, School of Basic Sciences, Jaipur National University, Jaipur, 302017, INDIA
*dwdpoonam@gmail.com

Abstract

In this study, biomolecules of the aqueous leaf extract of Azadirachta indica were used as a green catalyst for the synthesis of bimetallic- ZnO/MgO nanocomposites (ZM NCs). The function of biomolecules for the fabrication of biosynthesized ZM NCs was studied by FT-IR spectroscopy while the existence of both MgO and ZnO in ZM NCs was confirmed by SEM and TEM micrographs. Results of EDX spectroscopy with element mapping revealed the homogenous distribution of magnesium and zinc in the as-prepared nanocomposites. Powder XRD analysis reflects the polycrystalline nature of NCs with crystallite size ~33nm whereas XPS analysis confirmed the formation of ZnO-MgO heterojunction in ZnO/MgO NCs.

In addition, biosynthesized and characterized ZMNCs were evaluated for photodegradation performance using methylene blue solution (40ppm) under visible light irradiation. The achieved degradation efficiency of ZnO/MgO NCs (95.7%) was higher compared to biosynthesized monometallic nanoparticles {ZnO (82.4% and MgO (80.1%)}.

Keywords: *Azadirachta indica*, ZnO/MgO nanocomposites, XPS, Photodegradation, Methylene blue.

Introduction

Rapid growth of industries in last 5-6 decades and urbanization has created an adverse effect to environment because of disposal of wastes directly into water bodies and soil. Waste water effluent from industries contains a significant amount of heavy metals, organic pollutants and dyes that create surface and water pollution[27,28]. Among all, a huge amount of wastewater containing toxic and non biodegradable dyes from dying industries was used to dispose in water bodies which in turn contaminate surface and underground water[9]. Because of non-biodegradability, toxicity and high solubility in the aquatic environment, dyes can be easily absorbed by aquatic living species and are responsible for many diseases[22].

To solve this problem, various chemical techniques which include coagulation, membrane technology, ion-exchange, adsorption and photocatalytic degradation have been deployed to remove the dye from waste water[17,20]. Among all, photocatalytic degradation method proves itself superior to others because by this method dye molecules were used to decompose into nontoxic simple products in presence of semiconductor materials when irradiated with proper light. In this context, nanoparticles of metals and metal oxides play an effective role, as these nanomaterials possess advanced surface properties (due to Surface Plasmon resonance) in relation to bulk materials[1,10,14].

Many semiconductor materials such as ZnO, CuO, TiO_2, Ag, Fe_3O_4 and more have been reported as photocatalyst[2,19,29] by researchers. ZnO, being nontoxic, easily available and cost-effective material with band gap of 3.2, has been widely used by researchers but possesses rapid tendency to recombine photo-induced electron–hole pairs during degradation process. To minimize recombination, ZnO was doped with many metallic or nonmetallic materials such as CdS, CuO, Ag_2O, Ga and g-C_3N_4 and showed improved efficiency for photodegradation process[16,21,23,30]. MgO is a semiconductor material with a wide band gap and possesses unique physical and chemical properties[25]. As MgO is highly stable and has high pollutant adsorbent efficiency, it has been used as photocatalyst by many workers[5,13].

By reviewing literature, we have formed that nanoparticles are being fabricated by different physical and chemical methods such as hydrothermal, solution combustion, sol-gel, microwave, micro emulsion and more[3,18]. These methods have certain limitations viz. use of toxic chemicals, costly instrumentation, low yield and high temperature. Nowadays, synthesis of nanomaterials using biomaterials (algae, fungi, biomolecules and plant extract) is of great concern among researchers because of low cost, easy availability and utilization of non-toxic chemicals[7].

Considering different properties of ZnO and MgO in this study, we have reported the green and eco-friendly synthesis of ZnO/MgO nanocomposites (ZM NCs) using *Azadirachta indica* (*A. indica*) green leaves aqueous extract as a reducing and stabilizing agent. *A. indica* is a tree which belongs to family Meliaceae and is commonly found in India. It is a medicinal plant and has been used as medicine since ancient time in India. It is rich in phytochemicals including azadirachtins, nimbins, saponins, gallic acid, flavonoids, limonoids and more[24]. These biomolecules present in *A. indica* can act as non-toxic, green reducing and stabilizing agent during the preparation of nanoparticles.

In this study, an attempt has been made to understand the role of metabolites of green extract as a reducing and stabilizing agent for the fabrication of ZnO/MgO NCs.

Moreover, fabrication of green route synthesized ZM NCs was confirmed by different physicochemical techniques including FTIR, SEM, TEM, EDX, Powder XRD and XPS. Furthermore, biosynthesized ZM NCs have been evaluated for photocatalytic performance for the remediation of methylene blue solution in presence of visible light.

Material and Methods

Present research work was carried out by utilizing commercially received analytical grade chemicals (zinc acetate dihydrate from Thermo Fisher Scientific India Pvt. Ltd.; magnesium nitrate Thermo Fisher Scientific India Pvt. Ltd.; sodium hydroxide from Merck Life Science India Pvt. Ltd. and methylene blue from Merck Life Science India Pvt. Ltd.) without further purification. All solutions whenever required were prepared in deionised water throughout the experiment.

Preparation of *Azadirachta indica* (*A. indica*) leaf extract: *Azadirachta indica* green leaves were collected from Jaipur National University campus, India and then thoroughly washed under tap water to remove dust particles followed by drying in shade. The shade dried leaves were powdered by an electrical grinder and then 20 gm of leaf powder in 100 mL deionized water was refluxed using water condenser at 80^0C over a magnetic stirrer for 3 hours. Then after, suspension was cooled to room temperature and filtered using Whatmann's filter paper. The obtained filtrate (*A. indica* leaf extract) was stored in a refrigerator at 2^0C for further experimental study.

Biosynthesis of ZnO/MgO nanocomposites (ZM NCs): For *A. indica* green leaves mediated green synthesis of nanocomposites (NCs), equal volumes of precursors (0.1M magnesium nitrate and 0.1M zinc acetate solutions) were mixed in a 250 mL round bottom flask with continuous stirring. Then the resulting mixture solution was heated up to 80^0C followed by the addition of 40 mL of *A. indica* leaf extract. Then NaOH solution was added into the flask to maintain pH 10 and the resultant was stirred for 2 hours. As a result of this, colour of solution changed from light brown to blackish brown, indicating the fabrication of ZnO/MgO nanocomposites. Suspension was cooled to room temperature, centrifuged for 5 min at 8000 rpm and collected in a china dish. The product so formed was washed 5 times with ethanol to remove unconsumed NaOH and leaf extract, then dried in a hot air oven and finally calcined at 400^0C.

Biosynthesized sample was characterized by physico-chemical techniques including FT-IR, SEM and EDX with elemental mapping, TEM, XRD and XPS. Furthermore, bare MgO and ZnO nanoparticles had also been synthesized using *A. indica* green leaves to compare photocatalytic activity of MZ NCs with that of MgO or ZnO.

Experimentation for photocatalytic activity: The efficiency to degrade methylene blue (MB) solution (40ppm) as the model of organic pollutants by biosynthesized samples at pH 7 was evaluated in the presence of solar light irradiation for a period of 150 minute. For degradation study, three sets of five beakers (100 mL) with 30 mL of test solution (MB) and 5 mg of prepared sample (MgO, ZnO or ZnO/MgO) in each were prepared. All three sets were then irradiated with sunlight and after each interval of 30 min, one beaker from each set was removed from irradiation and evaluated for degradation by measuring the absorbance of solutions using UV-Vis spectrophotometer at $\lambda max = 665$ nm. The percentage of MB degradation was calculated by the formula:

$$\eta = (A_0 - A_t) / A_0 \times 100$$

where η represents degradation percentage and A_0 and A_t correspond to absorbance of MB dye solution at t = 0 and after time t respectively.

Characterization: FTIR spectral analysis was applied to understand the involvement of phytochemicals of *A. indica* green leaves extract in the fabrication of ZnO/MgO NCs and monometallic nanoparticles (MgO and ZnO). The study was carried out in the wavenumber range of 4000-400cm^{-1} using Perkin-Elmer spectrophotometer (MNIT, Jaipur). Surface morphology of ZM NCs was screened by Scanning electron microscopy and Transmission electron microscopy at MNIT, Jaipur. EDX analysis with elemental mapping was deployed to investigate the composition of elements in the nanocomposites. Purity and crystallinity of biosynthesized ZM NCs was examined by powder X-ray diffraction technique using PAN analytical (XPART PRO) diffractometer at 2θ values between 20^0- 80^0 using Cu Kα radiation (λ=1.5406Å). Chemical states of elements present in ZM NCs were analyzed at IIT, Roorkee using X-ray photoelectron spectroscopy (XPS, PHI 5000 Versa Probe III, IIT Roorkee).

Results and Discussion

FT-IR spectroscopic study: FTIR spectra of biosynthesized MgO and ZnO NPs along with ZnO/MgO NCs are showcased in fig. 1. In FTIR spectra of all three nano samples, some common absorption peaks appear at 3350-3460, 2980-2910, 1750-1700, 1450-1400, 1100-1080 cm^{-1} corresponding to stretching vibrations of O-H, C-H, aryl ketone, aromatic C=C and C-O functional groups respectively[7]. This showed that biomolecules present in *A. indica* green leaves extract containing phenolics and alcoholic groups in their structures had taken part in the formation of all nano products.

Occurrence of additional absorption peaks at 869.5 cm^{-1} and 562.7 cm^{-1} in the spectrum of MgO and ZnO is due to Mg-O and Zn-O stretching, respectively which supports the formation of monometallic MgO and ZnO nanoparticles[4]. However, in the spectrum of ZM NCs, Mg-O and Zn-O peaks shifted to lower wavenumber (866.9 cm^{-1} and 556.5 cm^{-1}) which confirmed the formation of ZnO/MgO nanocomposites.

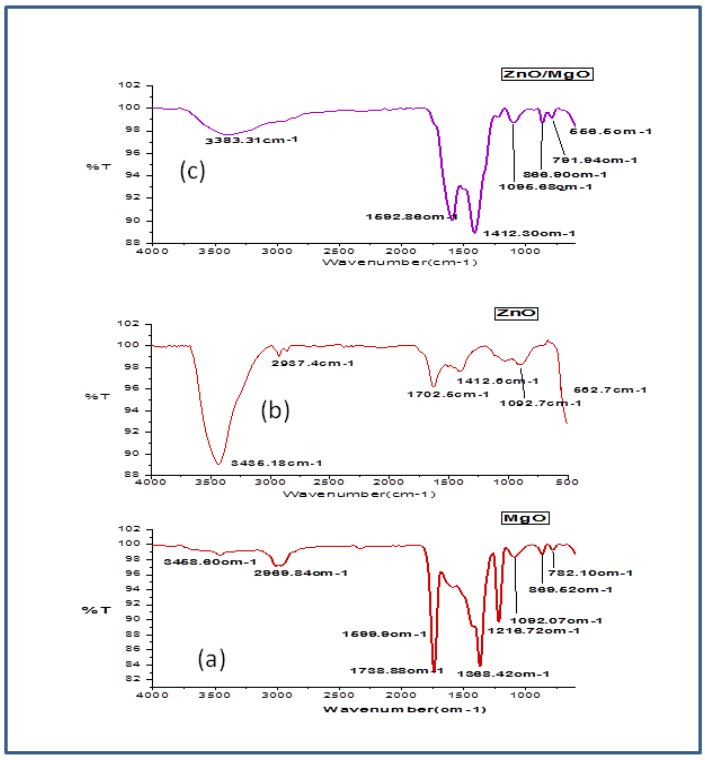

Figure 1: FTIR spectra of biosynthesized (a) MgO NPs (b) ZnO NPs (c)ZnO/MgO NCs

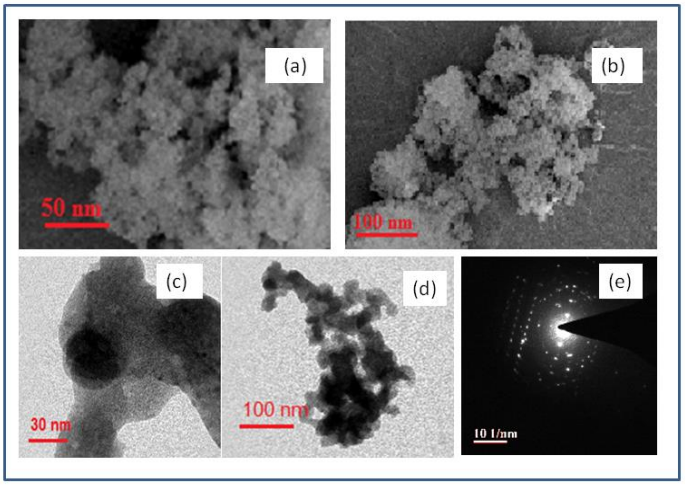

Figure 2: SEM images (a,b), TEM images (c,d) of ZnO/MgO NCs at different magnification and (e) SAED pattern of ZM NCs

Morphological study: Morphology of biosynthesized ZM NCs was screened by Scanning electron and transmission electron microscopic techniques (Fig. 2). SEM images of ZM NCs at different magnifications displayed in fig. 2(a,b) reveal that particles are of irregular cubic shape and appear as self associated with many nano-spheres of 20-60 nm range. Fig. 2 (c,d) depicts TEM images of bimetallic oxide NCs. It can be clearly seen from TEM micrographs that particles formed are of irregular spherical shape nano crystals with some capping agents. The presence of capping agents also indicates that some phytochemicals of extract were involved in fabrication of nanocomposites. Moreover, selected area electron diffraction (SAED) image of ZM NCs displayed in fig. 2(e) also interprets polycrystalline nature of the nanocomposites, which further infers the formation of bimetallic composites.

EDX and Elemental mapping: To determine the chemical composition of ZM NCs, EDX analysis with element mapping was also performed and results are displayed in figure 3. Strong peaks of Mg, Zn and O can be clearly seen in fig. 3(b) that further indicates the coexistence of MgO and ZnO. The appearance of carbon in the spectrum may be due to biomolecular capping on the surface of nano sample[12]. Elemental mapping images of ZM NCs are shown in figure 3 (c-f). It can be clearly seen from mapping images that Mg

and Zn are uniformly distributed in the composite. The existence of Mg, Zn and O in nanocomposites supports the formation of bimetallic mixed oxides.

Powder XRD study: Crystallinity and purity of biosynthesized ZM NCs were examined by using Powder X-ray diffraction analysis (XRD). Appearance of sharp peaks in diffraction pattern (Fig.4) reveals crystalline nature of as-prepared nanocomposites. Diffraction peaks at 2θ values 36.8°, 42.5°, 62.03°, 47.5°, 74.3° and 78.2 correspond to respective (111), (200), (220), (100), (110) and (222) crystallographic planes of cubic structured magnesium oxide in accordance to JCPDS file no. (89-7746) whereas existence of ZnO in green synthesized sample was illustrated by Bragg's peaks located at 31.8°, 34.5, 36.3°, 56.6°, 62.1°, 67.9° and 69.05°.

All these peaks are indexed to (100), (002), (101), (110), (103), (200) and (201) reflection planes of hexagonal wurtzite phased ZnO (JCPDS file no.89-1397). Any strong peak other than MgO or ZnO was not observed in the XRD pattern of ZM NCs. Furthermore, crystallite size at the most intense peak was calculated using Debye-Scherrer's formula[11] and found to be 33 nm. These outcomes of XRD study suggest the formation of pure and polycrystalline form of ZnO/MgO nanocomposites.

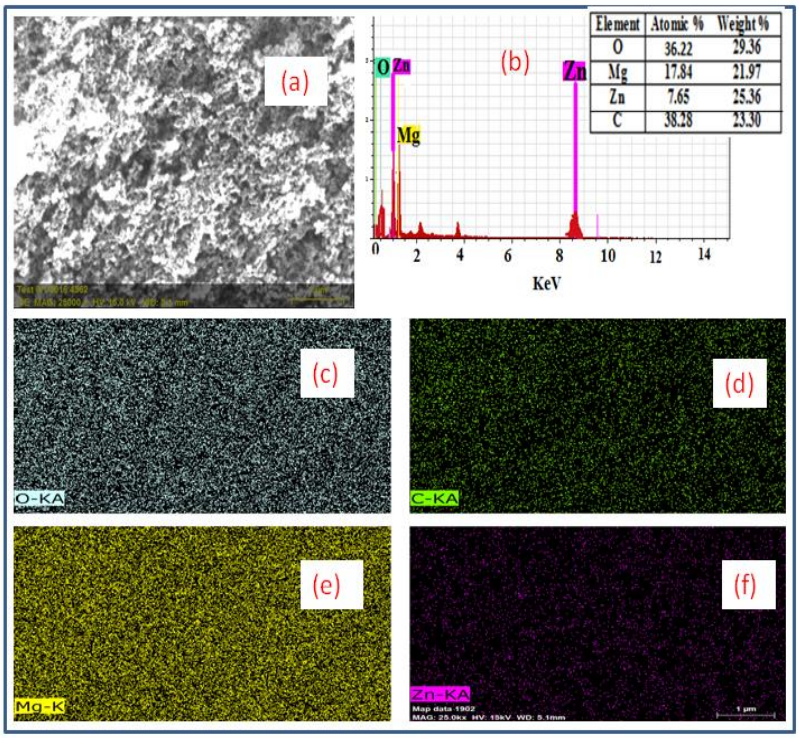

Figure 3: SEM image (a) EDX spectrum (b) and Elemental mapping (c-f) of ZnO/MgO nanocomposites

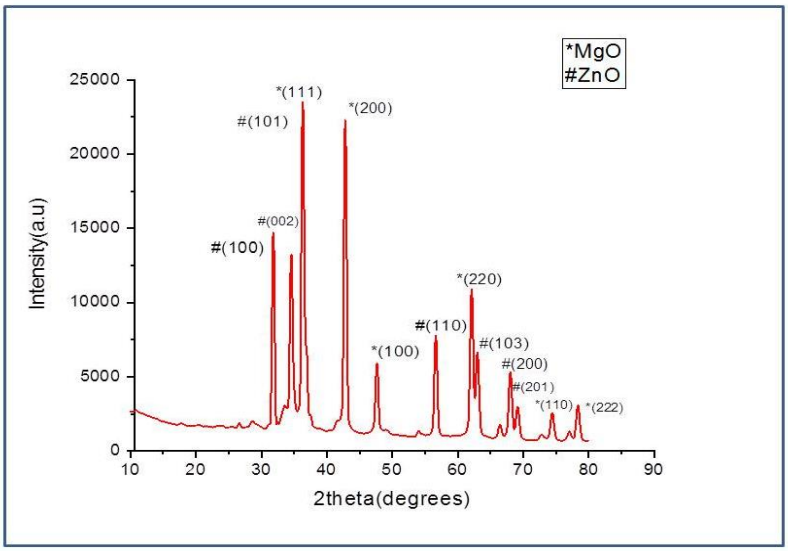

Figure 4: Powder XRD pattern of biosynthesized ZnO/MgO NCs

X-ray Photoelectron Spectroscopic (XPS) analysis: XPS study was carried out to analyze the chemical nature of the surface of as-prepared ZM NCs. Full scan spectra of ZM NCs are shown in figure 5(a) composed of Mg, Zn, O and C. High resolution XPS spectra of Mg2s, Mg2p, Zn2p, O1s and C1s are shown in fig. 5(b-e). In figure 5(b and c), peaks at binding energy 90.69 eV and 50.94 eV respective to Mg2s and Mg2p were observed which infer Mg^{2+} state of magnesium in ZnO/MgO[8]. In the Zn2p spectrum, two distinct peaks for $Zn2p_{3/2}$ and $Zn2p_{1/2}$ (spin-orbit doublet) were seen at binding energies 1023.5 eV and 1045.04 eV respectively (Fig. 5d). This suggests divalent oxidation state of zinc in ZnO/MgO composite[6]. The separation of two peaks of Zn2p by 21.54 eV supports nano-crystalline growth of ZnO/MgO. The presence of O1s at binding energy 530.68 eV (Figure 5e) indicated divalent (O^{-2}) state of oxygen in the sample[15].

In addition, HRXPS spectrum of C1s consists of two peaks at 284.6 eV(C=C)[31] and 286.8 eV (C=O)[26](Fig. 5f). These peaks of carbon might be due to hydrocarbons of biomolecules present in nanocomposites as capping agent. The outcomes of XPS study along with XRD results strongly support the formation of nano-size bimetallic oxides of zinc and magnesium.

Evaluation of photocatalytic activity: The photoremediation of MB in presence of green route processed- as-prepared nanoproducts (ZnO/MgO, ZnO and MgO) was examined under visible light and the magnitude of dye degradation was determined by measuring the absorbance of MB solution using a UV-Vis spectrophotometer. The results of degradation of MB solution by biosynthesized nanomaterials are displayed in figure 6 and table 1. Degradation outcomes revealed that bimetallic oxides nanocomposites possess more efficiency for MB degradation compared to monometallic nanoparticles (ZnO/MgO > ZnO > MgO). This remarkable increment in MB removal by ZnO/MgO NCs may be assigned to the synergistic effect between ZnO and MgO to degrade dye solution.

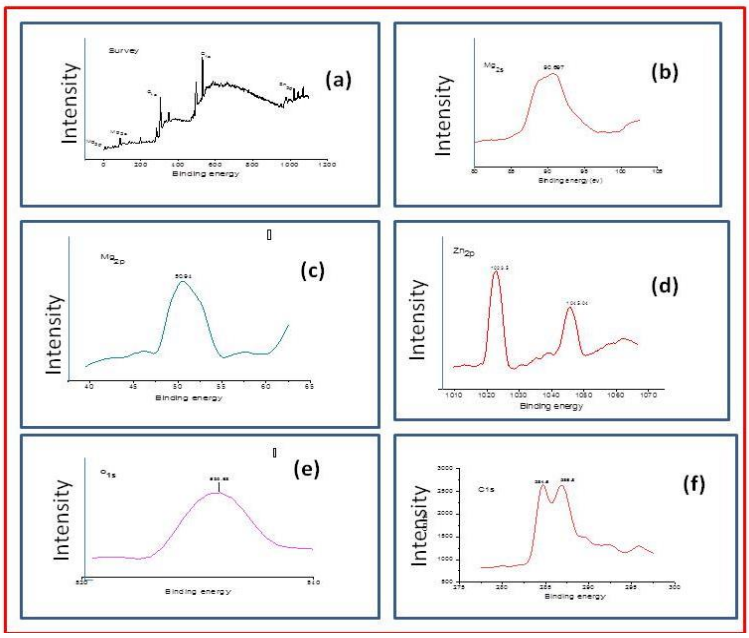

Figure 5: XPS spectra of ZnO/MgO NCs (a) Survey spectrum (b) Mg2s (c) Mg2p (d) Zn2p (e) O1s (f) C1s

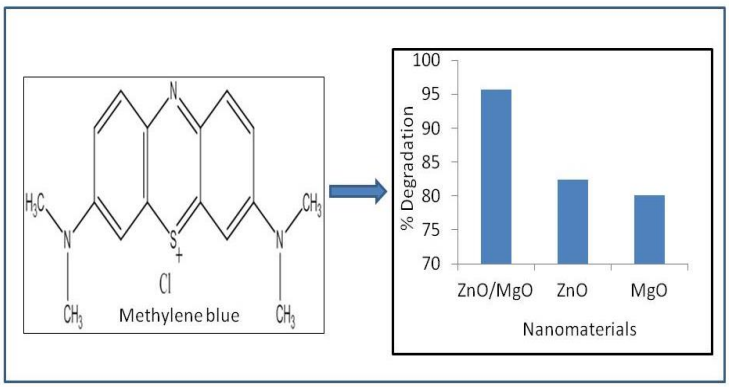

Figure 6: Graphical portrayal of % removal of MB in presence of *A. indica* leaves extract mediated nanomaterials

Table 1
Photoremediation of MB in presence of biosynthesized nanoproducts under solar light irradiation

Biosynthesized Nanomaterial	% degradation Time of MB (min)	
ZnO/MgO	95.7	150
ZnO	82.4	150
MgO	80.1	150

Conclusion

In summary, an eco-friendly, cost-effective and green procedure has been used for the successful synthesis of ZnO/MgO nanocomposites. FTIR analysis revealed the role of biomolecules of *A.indica* leaf extract in reducing and capping of zinc and magnesium ions to fabricate ZM NCs. Existence of Mg and Zn in composite material was confirmed successfully by SEM, TEM and EDX analysis. Elemental mapping study showed the homogeneous distribution of magnesium and zinc in the composite. XPS outcomes revealed the formation of Zn-Mg hetero-junction in ZnO/MgO NCs while XRD results illustrated the polycrystalline nature of nanoparticles.

In addition, photocatalytic efficacy of ZnO/MgO NCs along with monometallic nanoparticles (ZnO and MgO) was evaluated for the degradation of methylene blue solution under visible light irradiation and observations revealed that ZM NCs have greater potency than ZnO or MgO NPs. Thus, this study reveals that *A.indica* leaf extract synthesized ZnO/MgO NCs has more potential than respective ZnO or MgO nanoparticles and can be used for environmental remediation in the future.

Acknowledgement

The authors would like to thank Chancellor, Jaipur National University, Jaipur, India for providing laboratory facilities to this work.

References

1. Aarthi T. and Madras G., Photocatalytic Degradation of Rhodamine Dyes with Nano-TiO_2, *Ind Eng Chem Res*., **46(1)**, 7–14 **(2007)**

2. Anjum M., Miandad R., Waqas M., Gehany F. and Barakat M.A., Remediation of waste water using various nano-materials, *Arab J Chem*., **12(8)**, 4897–919 **(2019)**

3. Arya S., Mahajan P., Mahajan S., Khosla A., Datt R., Gupta V., Young S.J. and Oruganti S.K., Review—Influence of Processing Parameters to Control Morphology and Optical Properties of Sol-Gel Synthesized ZnO Nanoparticles, *ECS J. Solid State Sci. Technol.*, **10**, 023002 **(2021)**

4. Baranov A.N., Kapitanova O.O., Panin G.N. and Kang T.V., Russ. J., ZnO/MgO nanocomposites Generated from Alcoholic Solutions, *Inorg. Chem*., **53**, 1366 – 70 **(2008)**

5. Cai Y., Li C., Wu D., Wang W., Tan F., Wang X., Wong P.K. and Qia X., Highly active MgO nanoparticles for simultaneous bacterial inactivation and heavy metal removal from aqueous solution, *Chem. Eng. J*., **312**, 158–166 **(2017)**

6. Chen J.T., Wang J., Zhuo R.F., Yan D., Feng J.J., Zhang F. and Yan P.X., The effect of Al doping on the morphology and optical property of ZnO nanostructures prepared by hydrothermal process, *Appl Surf Sci*, **255**, 3959-64 **(2009)**

7. Dwivedi P., Jatrana I., Khan A.U., Khan A.A., Satiya H., Khan M., Moon I.S. and Alam M., Photoremediation of methylene blue by biosynthesized ZnO/Fe3O4 nanocomposites using Callistemon viminalis leaves aqueous extract: A comparative study, *Nanotech Rev.*, **2(10)**,1912–25 **(2021)**

8. Hassan S.E.D., Fouda A., Saied E., Farag M.M.S., Eid A.M., Barghoth M.G., Awad M.A., Hamza M.F. and Awad M.F., Rhizopus oryzae-Mediated Green Synthesis of Magnesium Oxide Nanoparticles (MgO-NPs): A Promising Tool for Antimicrobial, Mosquitocidal Action and Tanning Effluent Treatment, *J. Fungi*, **7**, 372 **(2021)**

9. He C., Yu Y., Hu X. and Larbot A., Influence of silver doping on the photocatalytic activity of titania films, *Appl Surf Sci*., **200(1–4)**, 239–47 **(2002)**

10. Jena M., Manjunatha C., Shivaraj B.W., Nagaraju G., Ashoka S. and Aan M.P.S., Optimization of parameters for maximizing photocatalytic behaviour of $Zn_{1-x}Fe_xO$ nanoparticles for methyl orange degradation using Taguchi and Grey relational analysis Approach, *Mater. Today Chem*., **12**, 187-199 **(2019)**

11. Joghee S., Pradheesh G., Alexramani V., Sundrarajan M. and Hong S., Green synthesis and characterization of zinc oxide nanoparticle using insulin plant (Costus pictusD.Don) and investigation of its antimicrobial as well as anticancer activities, *Adv. Nat. Sci: Nanosci. Nanotechnol*., **9**, 015008 **(2018)**

12. Karthikeyan B. and Loganathan B., Rapid green synthetic protocol for novel trimetallic nanoparticles, *J Nanoparticles*, **2013,** 8 **(2013)**

13. Khan A., Shabir D., Ahmad P., Khandaker M.U., Faruque M.R.I. and Uddin I., Biosynthesis and antibacterial activity of MgO-NPs produced from Camellia-sinensis leaves extract, *Mater. Res. Express*, **8**, 015402 **(2020)**

14. Kumar S.G. and Rao K.S.R.K., Tungsten-based nanomaterials (WO3 and Bi2WO6): Modifications related to charge carrier transfer mechanisms and photocatalytic applications, *Appl Surf Sci*., **355**, 939–58 **(2015)**

15. Kumar V. et al, Synthesis of CuO and Cu2O nano/microparticles from a single precursor: effect of temperature on CuO/Cu2O formation and morphology dependent nitroarene reduction, *RSC Adv*., **6**, 85083-90 **(2016)**

16. Kundu P., Deshpande P.A., Madras G. and Ravishankar N., Nanoscale ZnO/CdS heterostructures with engineered interfaces

for high photocatalytic activity under solar radiation, *J Mater Chem*., **21(12)**, 4209–16 **(2011)**

17. López C., Valade A.G., Combourieu B., Mielgo I., Bouchon B. and Lema J.M., Mechanism of enzymatic degradation of the azo dye Orange II determined by ex situ 1H nuclear magnetic resonance and electrospray ionization-ion trap mass spectrometry, *Anal Biochem*., **335(1)**, 135–49 **(2004)**

18. Manjunatha C., Ashoka S. and Hari Krishna R., Elsevier, Microwave-assisted green synthesis of inorganic nanomaterials, Elsevier, eBook **(2020)**

19. Manjunatha C., Abhishek B., Shivaraj B.W., Ashoka S., Shashank M. and Nagaraju G., Engineering the MxZn1−xO (M = Al3+, Fe3+, Cr3+) nanoparticles for visible light-assisted catalytic mineralization of methylene blue dye using Taguchi design, *Chem. Pap*., **74**, 2719-2731 **(2020)**

20. Nagaveni K., Hegde M., Ravishankar N., Subbanna G. and Madras G., Synthesis and Structure of Nanocrystalline TiO_2 with Lower Band Gap Showing High Photocatalytic Activity, *Langmuir*, **20(7)**, 2900–7 **(2004)**

21. Nagendra G.K., Shivaraj B.W., Manjunatha C., Siddiqua S.A.A. and Suchithra V., Study of structural features and antibacterial property of ZnO/CuO nanocomposites derived from solution combustion synthesis, IOP Conf. Ser.: Mater. Sci. Eng., **577**, 012111 **(2019)**

22. Nilsson I., Möller A., Mattiasson B., Rubindamayugi M.S. and Welander U., Decolorization of synthetic and real textile wastewater by the use of white-rot fungi Enzyme, *Microb Technol*., **38(1–2)**, 94–100 **(2006)**

23. Pal S., Maiti S., Maiti U.N. and Chattopadhyay K.C., Low temperature solution processed ZnO/CuO heterojunction photocatalyst for visible light induced photo-degradation of organic pollutants, *Cryst. Eng. Comm*., **17(6)**, 1464–76 **(2015)**

24. Pandey G., Verma K.K. and Singh M., Evaluation of phytochemical, antibacterial and free radical scavenging properties of azadirachta indica (neem) leaves, *Int. J. Pharm. Pharm*., **6(2)**, 444-447 **(2014)**

25. Ramanujam K. and Sundrarajan M., Antibacterial effects of biosynthesized MgO nanoparticles using ethanolic fruit exract of Emblica officinalis, *J Photochem Photobiol B*., **141**, 296–300 **(2014)**

26. Sahu S.K., Chakrabarty A., Bhattacharya D., Ghosh S.K. and Pramanik P., Single step surface modification of highly stable magnetic nanoparticles for purification of His-tag proteins, *J Nanopart Res*., **13(6)**, 2475–84 **(2011)**

27. Sörme L. and Lagerkvist R., Sources of Heavy Metals in Urban Wastewater in Stockholm, *Sci. Total Environ*., **298**, 131–45 **(2002)**

28. Srivastava V.C., Mall I.D. and Mishra I.M., Characterization of Mesoporous Rice Husk Ash (RHA) and Adsorption Kinetics of Metal Ions from Aqueous Solution onto RHA, *J. Hazard Mater.*, **134**, 257–67 **(2006)**

29. Vidya C., Manjunatha C., Handraprabha M., Rajshekar M. and Raj M.A.L.A., Hazard free green synthesis of ZnO nano-photo-catalyst using Artocarpus Heterophyllus leaf extract for the degradation of Congo red dye in water treatment applications, *J. Environ. Chem. Eng.*, **5(4)**, 3172-3180 **(2017)**

30. Young S.J., Liu Y.H., Shiblee M.D.N.I., Ahmed K., Lai L.T., Nagahara L., Thundat T., Yoshida T., Arya S., Furukawa H. and Khosla A., Flexible Ultraviolet Photodetectors Based on One-Dimensional Gallium-Doped Zinc Oxide Nanostructures, *ACS Appl. Electron. Mater*., **2**, 3522−3529 **(2020)**

31. Zhan S., Zhu D., Ma S., Yu W., Jia Y., Li Y., Yu H. and Shen Z., Highly efficient removal of pathogenic bacteria with magnetic graphene composite, *ACS. Appl. Mater. Interfaces*, **7**, 4290–4298 **(2015)**.

(Received 25th July 2022, accepted 30th September 2022)